Bioorganic Chemistry 90 (2019) 103047

Contents lists available at ScienceDirect

Bioorganic Chemistry

journal homepage: www.elsevier.com/locate/bioorg

A competent synthesis and efficient anti-inflammatory responses of isatinimino acridinedione moiety *via* suppression of *in vivo* NF-κB, COX-2 and iNOS signaling

Govindasami Periyasami[a,*], Paulrayer Antonisamy[b], Karthikeyan Perumal[c], Antony Stalin[d], Mostafizur Rahaman[a], Asma A. Alothman[a]

[a] Department of Chemistry, College of Science, King Saud University, Riyadh 11451, Saudi Arabia
[b] Department of Korean Physiology, Wonkwang University School of Korean Medicine, 460 Iksan-daero, Iksan City, Jeonbuk 570-749, Republic of Korea
[c] Department of Chemistry, The Ohio State University, 170A CBEC, 151 West Woodruff Avenue, Columbus, OH 43210, United States
[d] Department of Traditional Chinese Medicine, Zhejiang A&F University, Hangzhou 311300, China

ARTICLE INFO

Keywords:
Anti-inflammatory
Paw oedema
Carrageenan
Acridinedione
COX-2
iNOS
NF-kB
In silico docking
5F19 receptor

ABSTRACT

A potent Nonsterodial Anti-inflammatory Drug (NSAID) candidates has been conceived and built by an assembly of a hydrophilic, fluorescent and COX-2 inhibiting units in the same molecule. The isatinimino-acridinedione core (**TM-7**) was achieved in a simple three step synthetic procedure *viz* (i) a multicomponent reaction between dimedone, aldehyde and amine to furnish the nitroacridinedione (**4**), (ii) reduction step and (iii) schiff's-base condensation with isatin. The excellent anti-inflammatory pharmacological efficiency of the drug was established by *in vivo* biological experiments. Accordingly, it was found that the treatment with the synthesized isatinimino analogues (dosage: 30 mg/kg) inhibited protein expression of cyclooxygenase-2 (COX-2), inducible nitric oxide synthase (iNOS), and nuclear factor kappa B (NF-κB) as well as production of prostaglandin E2 (PGE2), nitric oxide (NO), tumor necrosis factor-alpha (TNF-α), interleukin-1beta (IL-1β), and interleukin-6 (IL-6) levels induced by carrageenan. Further, a comparative molecular modeling analysis of TM-7 carried out with the crystal structure of aspirin acetylated human COX-2 suggested effectively binding and efficient accommodation inside the active site's gorge.

1. Introduction

Inflammation is a normal physiological reaction of the body against invading pathogens, which is normally identified by redness, swelling, pain, and heat. A lot of scientific studies have delivered proof that inflammation is involved in the pathogenesis of several diseases including cancer [1], aging [2], cardiovascular dysfunction [3], and other life-threatening and devastating disorders. Acute inflammation is a process that involves a significant production of several inflammatory and pro-inflammatory mediators, free radicals, and activation of complex enzymes. Carrageenan-induced paw oedema study is a well-known acute inflammation model commonly used for testing novel anti-inflammatory drugs. Following this procedure, biphasic oedema is induced in the sub-plantar surface of rat hind paw by injecting Carrageenan. The early phase is associated with the release of histamine, bradykinin, serotonin, and prostaglandins (PGs) produced by cyclooxygenase enzymes (COX), while the delayed phase contributes to neutrophil infiltration, and the ongoing production of PGs [4]. The delayed phase of carrageenan-induced acute inflammation also releases neutrophil-derived reactive oxygen species (ROS), nitric oxide (NO), and pro-inflammatory cytokines including interleukin-1 β (IL-1 β) and tumor necrosis factor (TNF-α) [5]. Diverse scientific reports have suggested that drugs targeting the COX enzyme, pro-inflammatory protein expression (e.g. inducible nitric oxide synthase (iNOS)), and free radical formation might deliver significant anti-inflammatory effects than the currently available therapeutic agents [6]. In this regard, the present study aims to provide the evaluation of anti-inflammatory activity of a newly synthesized isatinimino acridiendione molecule, along with a brief discussion on its synthetic chemistry.

Acridinedione motifs continue to receive substantial attention from various biological and biomedical fronts including photodynamic therapy [7]. This can be attributed to their broad spectrum of pharmaceutical properties such that antitumor [8], antimalarial [9], antiprotozoal [10], antileukemic [11], antinociceptive [12], and anti-

* Corresponding author.
E-mail address: pkandhan@ksu.edu.sa (G. Periyasami).

https://doi.org/10.1016/j.bioorg.2019.103047
Received 17 March 2019; Received in revised form 28 May 2019; Accepted 5 June 2019
Available online 11 June 2019
0045-2068/

inflammatory properties [13]. Owing to the structural similarity of acridinedione core unit with 1,4-dihydropyridine, and biologically important co-enzyme Nicotinamide adenine dinucleotide (NADH), it has recently acquired rejuvenated importance in the field of biomedical research. Moreover, due to the bi-chromophoric property of acridinedione dyes, it has been demonstrated that by judicious variation of substitution groups at the 9th and/or 10th positions, they can be modified as ideal fluorescent probe for proteins [14], hydrogen-bonding assemblies [15,16] and also fluorescent sensors [17,18]. Also, 9-aryl substituted acridinedione analogues have been used as an effective vascular potassium channel openers. Apart from this, acridine-1,8-dione analogues have been reported as novel GCN5 inhibitors that are involved in metabolic disorders and cancer progression, particularly, in colon cancer and lung cancer. Collectively, the substituted acridinedione motif has evidence in the literature as an attractive and efficient target for therapeutic applications. However, the reported therapeutic applications of acridinedione against inflammation activity are limited and it remains an essential goal in medicinal chemistry.

Inspiringly, hybrid small molecules composed of NSAIDs are more efficient, in terms of potency, time consumption, and possibly may have less side effects compared with the commercially available anti-inflammatory drugs [19]. Herein, we report the design and synthesis of a low molecular weight acridine-1,8-dione hybrid containing a broad spectrum of enzyme inhibiting substitutions such as the isatin analogue, linked as 3-(phenylimino)indolin-2-one at the 10th position and phenolic substitution at the 9th position as a hydrophilic unit. Obtaining amide functionality in isatin has shown a broad range of biological properties [20], including anti-HIV [21], anti-cancer [22], and anti-inflammatory properties [23]. Interestingly, the amide group is a great alternative for the carboxylic groups in NSAID drugs, for example, indomethacin, meclofenamic acid, and ketoprofen showed greater selectivity for COX-2 enzyme [24]. We anticipated that, the ability of the designed compound will have a broad spectrum of fluorescent emission due to the bichromophoric nature of the central acridine-1,8-dione unit and also it can inhibit the COX-2 enzyme as well as it can easily pass-through protein channels due to the presence of the hydrophilic phenolic unit.

2. Results and discussion

2.1. Chemistry

Acridine-1,8-dione bridged NSAID-COX inhibitor synthesis

The current research endeavor envisions the synthesis and an *in vivo* evaluation of anti-inflammatory nature of a fluorescent dye unit spacer containing a COX-2 inhibitor decorated with a lipophilic substitution obtained by an easily accessible and efficient procedure. Hence, the drug target was proposedly designed as small molecular hybrids containing a selective NSAID (COX inhibitor) inhibitor amide group, and a lipophilic phenolic group linked through an acridine-1,8-dione dye center unit in a 1:1 ratio (Fig. 1). We hypothesized that the isatin amide functionality may compete as good as the COOH moiety for efficient COX inhibition and will therefore usher good anti-inflammatory activity. In Scheme 1, the retro synthetic analysis, which directed us to the possible synthetic route to achieve the target molecule is described.

In path A, the most prominent direct Hantzsch reaction may produce dimeric acridiendione due to the presence of two aromatic amine groups present in *m*-phenylenediamine, and it will not be suitable for further Schiff condensation with an isatin moiety. Path B offers the advantage of being an easy one step method; however, a report from Wang et al. [25] suggests that the imine group of the 2-indolinone imino-amine might also involve in the cyclization and therefore it may not retain in the final product. Hence, path C was perceived to be an appropriate synthetic route to obtain the desired product.

Initially, the required precursor tetraketone was synthesized through a Knoevenagel condensation followed by a Michael addition

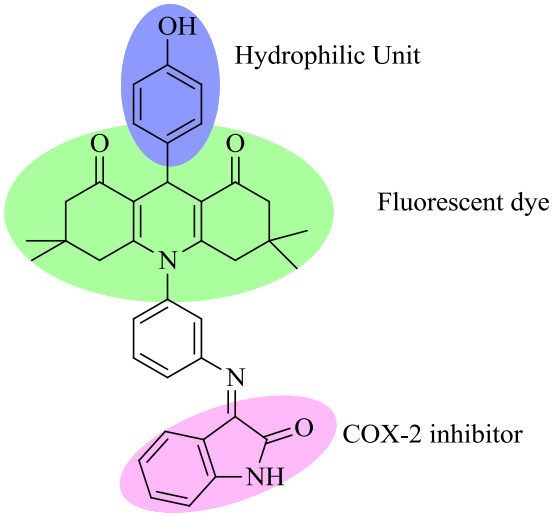

Fig. 1. Structure of the acridine-1,8-dione dye core NSAID-COXs inhibitor.

reaction between 4-hydroxy benzaldehyde (**1**) and dimedone (**2**). Further the generated tetraketone underwent cyclization with 3-nitroaniline (**3**) at room temperature in EtOH/H_2O (1:1) with a catalytic amount of acetic acid as a solvent. The yielded crude nitroacridinedione (**4**) was purified by a filter column, and the product was further treated with a reducing agent such as Fe powder with ammonium chloride to furnish the corresponding aminoacridine-1,8-dione (**5**) in good yield. The synthetic route of amine functionalized acridinedione is illustrated in Scheme 2.

As depicted in Scheme 3, the target molecule (TM) isatinimine acridinedione (TM-**7**) was synthesized through Schiff base condensation methodology by refluxing equimolar quantities of aminoacridinedione (**5**) and isatin (**6**) in ethanol with a catalytic amount of acetic acid. The reaction completion was monitored by TLC, and the crude product was purified through flash silica gel column chromatography.

The structure of the product TM-7 was confirmed by their spectral data. In the FT-IR spectrum of TM-7, two broad stretching vibrational absorption bands were found to appear at 3427 cm^{-1} and 3382 cm^{-1} corresponding to aromatic OH and iminooxindole amide NH respectively. A sharp absorption band observed at 1736 cm^{-1} corresponds to carbonyl groups of acridinedione and the amide carbonyl of iminooxindole exhibited a sharp band at 1716 cm^{-1}. Aromatic and aliphatic C—H stretching bands were observed at 3121 cm^{-1} and 2955 cm^{-1} respectively. A band which appeared at 1618 cm^{-1} was assigned to imine C═N stretching frequency. The ^{1}H NMR spectrum showed one proton singlet at δ 4.88 ppm corresponding to benzylic CH and the aromatic protons resonated as multiplets in the region between δ 6.51–7.36. In the ^{13}C DEPT-135 spectrum, two intense signals appeared in the negative region corresponding to the methylene carbons present in the compound. Further, the ^{13}C NMR spectrum of TM-7, displayed oxindole carbonyl carbon resonances at 163.82 ppm and that of the acridinedione carbonyl carbon at 195.62 ppm. The assignment of carbon signal at 163.8 ppm support the presence of imine carbon in the target molecule. The NMR spectra of synthesized compounds are presented in Electronic Supplementary Information (ESI). In addition, the mass spectrum (ESI-MS) of TM-7 exhibited the molecular ion peak at *m/z* 585.28 corresponding to the molecular mass of TM-7. The compound also gave satisfactory results from elemental analysis.

2.2. In vivo anti-inflammatory studies

The Carrageenan-induced hind paw edema is a well-known model of acute inflammation involving a variety of inflammatory mediators and has widely been used to assess the anti-inflammatory effect of new

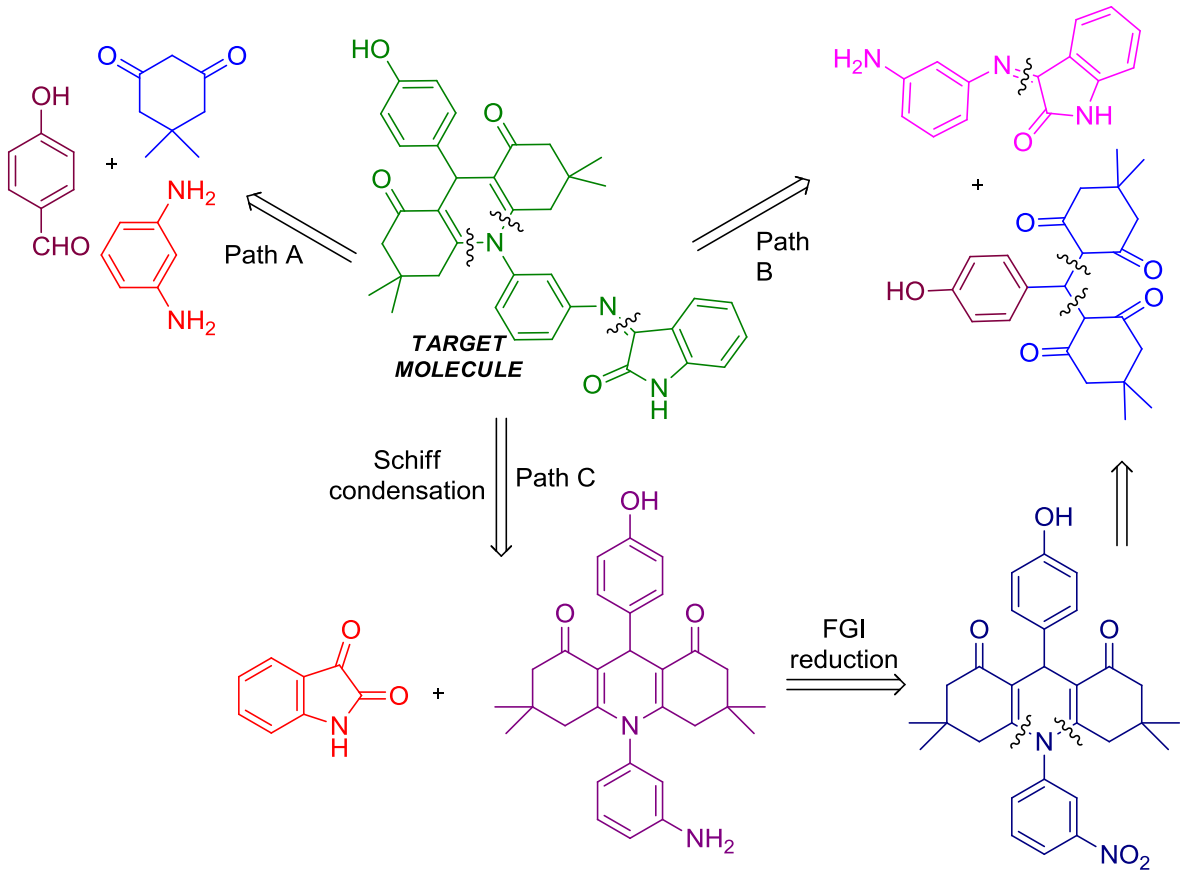

Scheme 1. The retrosynthetic approach for the synthesis of acridine-1,8-dione dye bridged NSAID-COX inhibitor.

drugs. The macroscopic appearance and paw oedema inhibition of indomethacin and the test TM-7 against carrageenan-induced hind paw oedema are shown in Fig. 2. Indomethacin and the tested TM-7 showed 52.02% and 53.13% inhibition of inflammation at the 5th hour when compared to the control (Fig. 3).

The TM-7 significantly inhibited TNF-α (1.62 fold), IL-1β (2.94 fold), and IL-6 (2.38 fold) levels similar to indomethacin TNF-α (1.58 fold), IL-1β (2.60 fold), and IL-6 (2.45 fold) (Fig. 4**A–C**). PGE2 (1.57 fold) and nitrite levels (1.88 fold) were significantly decreased by the treatment of TM-7 compared to the control group (Fig. 5**A and B**). In order to identify whether the anti-inflammatory activity of TM-7 was reasonable due to its antioxidant activity, the hepatoprotective properties of TM-7 were evaluated by malondialdehyde (MDA) level measurement as an index of lipid peroxidation. As shown in Fig. 5**C**, the MDA level significantly increased (2.39 fold) in liver tissue of rats at the 5th hour after carrageenan injection. On the other hand, the MDA level was declined significantly (2.17 fold) by treatment with TM-7. Indomethacin produced significant inhibition on the MDA level similar to compound **7**. MDA is a metabolic product of lipid peroxidation and its level is expected to rise during oxidative stress. The current results displayed that TM-7 (30 mg/kg) reduce the severity of liver damage by decreasing the MDA levels. A growing body of evidence proposes the anti-oxidative effect of TM-7, which is consistent with previous reports [26].

Expression of COX-2, iNOS, and proinflammatory cytokines are known to be regulated by NF-κB at the transcriptional level [27]. In the present study, treatment with TM-7 (30 mg/kg) resulted in a significant reduction of iNOS (1.71 fold), COX-2 (2.15 fold), and NF-κB (2.14 fold) protein expressions in carrageenan-induced hind paw oedema indicating that TM-7 could inhibit iNOS, COX-2 expression through the

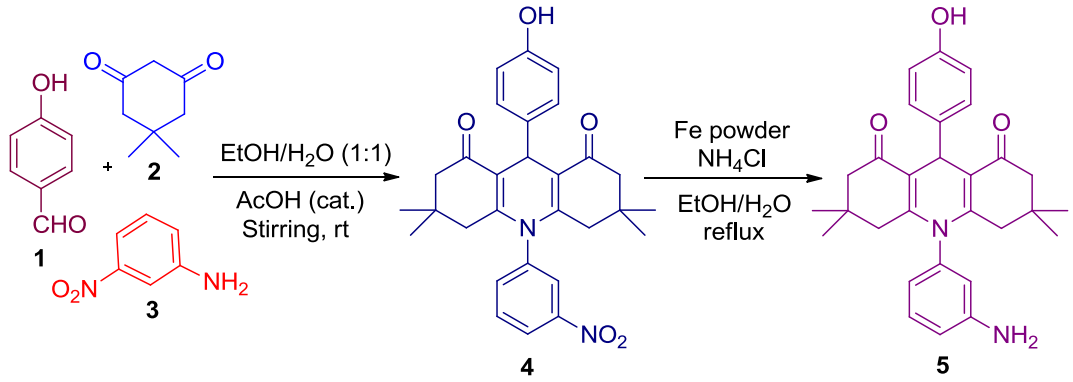

Scheme 2. Synthesis of acridine-1,8-dione amine (**5**).

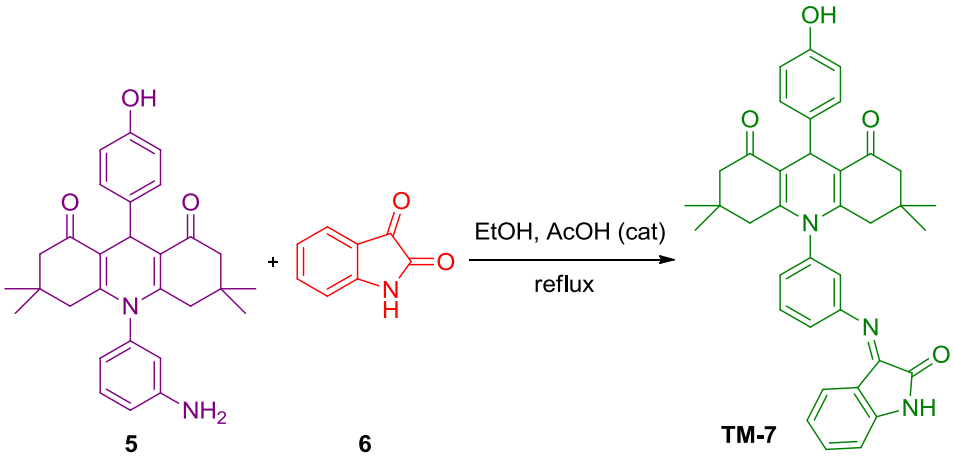

Scheme 3. Synthesis of target molecule **TM-7** through Schiff base condensation of amine (**5**) and isatin (**6**).

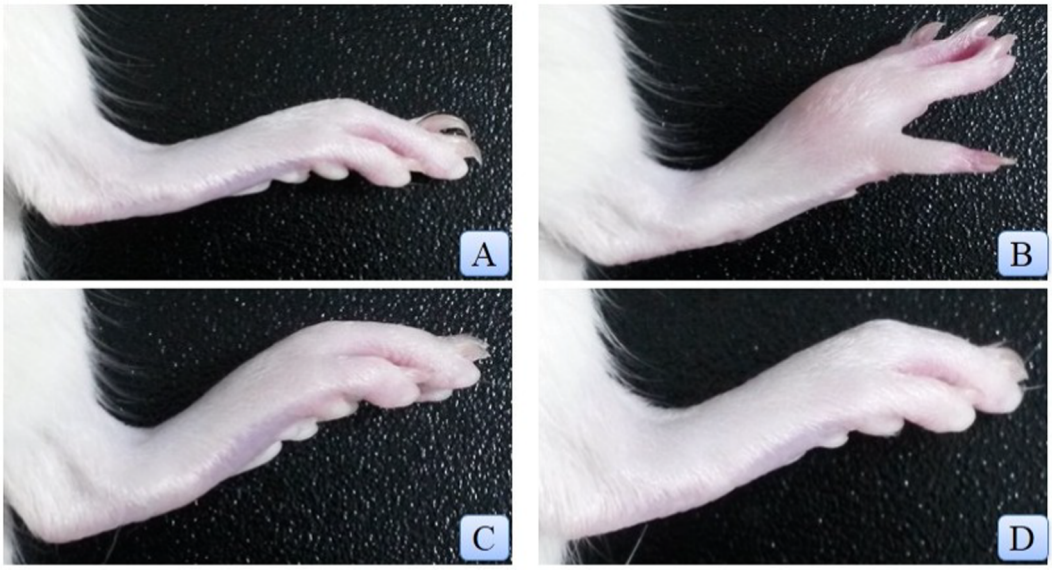

Fig. 2. Macroscopic images of carrageenan-induced hind paw oedema and the anti-inflammatory effect of TM-7 (30 mg/kg) and indomethacin (10 mg/kg). (A) Normal control; (B) control; (C) TM-7 (30 mg/kg); and (D) indomethacin (10 mg/kg).

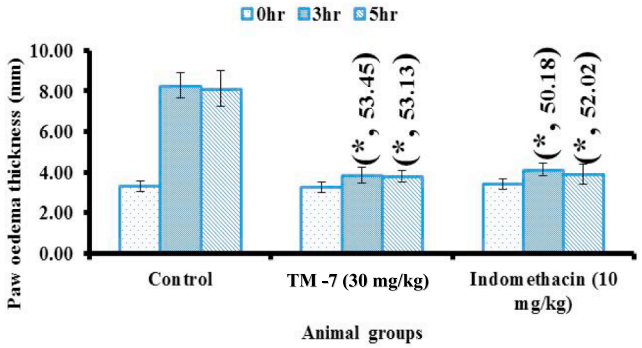

Fig. 3. Effect of TM-7 (30 mg/kg) and indomethacin (10 mg/kg) on carrageenan induced hind paw oedema in rats.

suppression of NF-κB (Fig. 6**A–D**). In order to evaluate the transudative, exudative, and proliferative components of subacute inflammation, we have applied the cotton pellet induced granuloma method. The results are shown in Fig. 7. TM-7 (30 mg/kg) and standard drug (indomethacin 10 mg/kg) elicited a significant inhibitory activity on the wet weight of granuloma.

2.3. Docking simulation

To validate the ligand-receptor associations, TM-7 was selected for docking studies and the commercially available anti-inflammatory drug Indometacin as the reference compound for comparative study. We anticipated that it may provide insights on binding possibilities with lower binding energy through docking with receptor COX-2 (5F19). The synthesized COX-2 inhibiting TM-7 molecule was subjected to docking experiments in order to elucidate its anti-inflammatory response. We expected that it can activate the molecules due to their presence for hydrophilic unit. The results of the docking experiment of the selected ligand TM-7 with 5F19 showed efficient interactions with the active amino acids in the active site pocket. The binding interaction with the amino acid residues THR‘60/O, ARG‘61/HE, SER‘121/O, LYS‘532/HZ2 were identified in the least energy value (−8.82 kcal/mol). Notably, the values closely matched with the binding energy of Indomethacin (−8.98 kcal/mol). having interaction with amino acids receptors CYS‘47/HN, TYR‘130/HH, LYS‘137/HZ1, GLN‘461/2HE2 in the active pocket. Further, the inhibition constant and ligand efficiency of TM-7 (341.7 nM) is significantly better than with reference drug indomethacin (263.12 nM). Since TM-7 showed the binding interaction with the different amino acids but in the same active pocket like that of

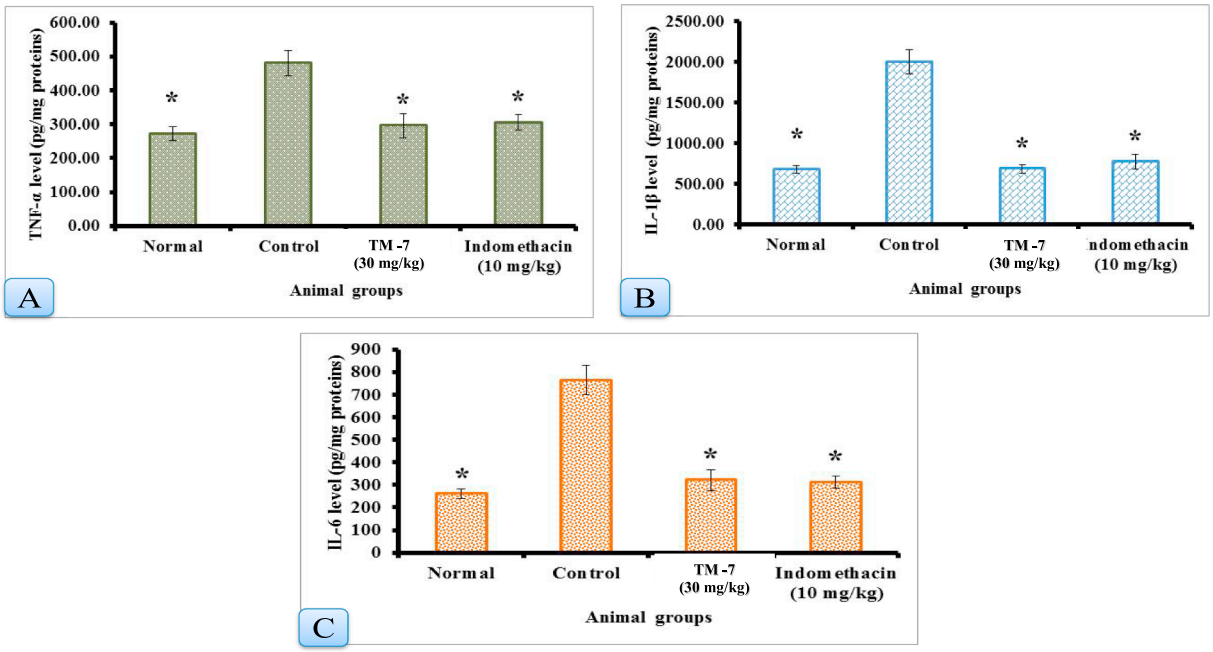

Fig. 4. Effect of TM-7 (30 mg/kg) and indomethacin (10 mg/kg) on TNF-α, IL-1β, and IL-6 levels.

Indomethacin, and comparable to the crystal structure of aspirin acetylated human cyclooxygenase-2 [28]. Furthermore, the *in vivo* study of our synthesized target showed the significant inhibition against COX-2. Additionally, the TM-7 has been well packed in the active pocket of COX-2 structure and it represents the strong binding interaction with the active amino acids [29]. Hence, it is apparent that the TM-7 might be develop a new inhibition pathway and act as a novel inhibitor for COX-2 and its associated enzymes. The docking results are shown in Table 1 also Figs. 8 and 9 represented the 3D picture and 2D interaction diagram of the corresponding binding conformations of TM-7 and Indomethacin has been presented respectively.

3. Experimental

3.1. Synthesis of nitro substituted acridinedione **4**

5,5-Dimethylcyclohexane-1,3-dione (2 equiv) was dissolved in 20 mL EtOH/H_2O (1:1) and then 4-hydroxybenzaldehyde (1 equiv) was

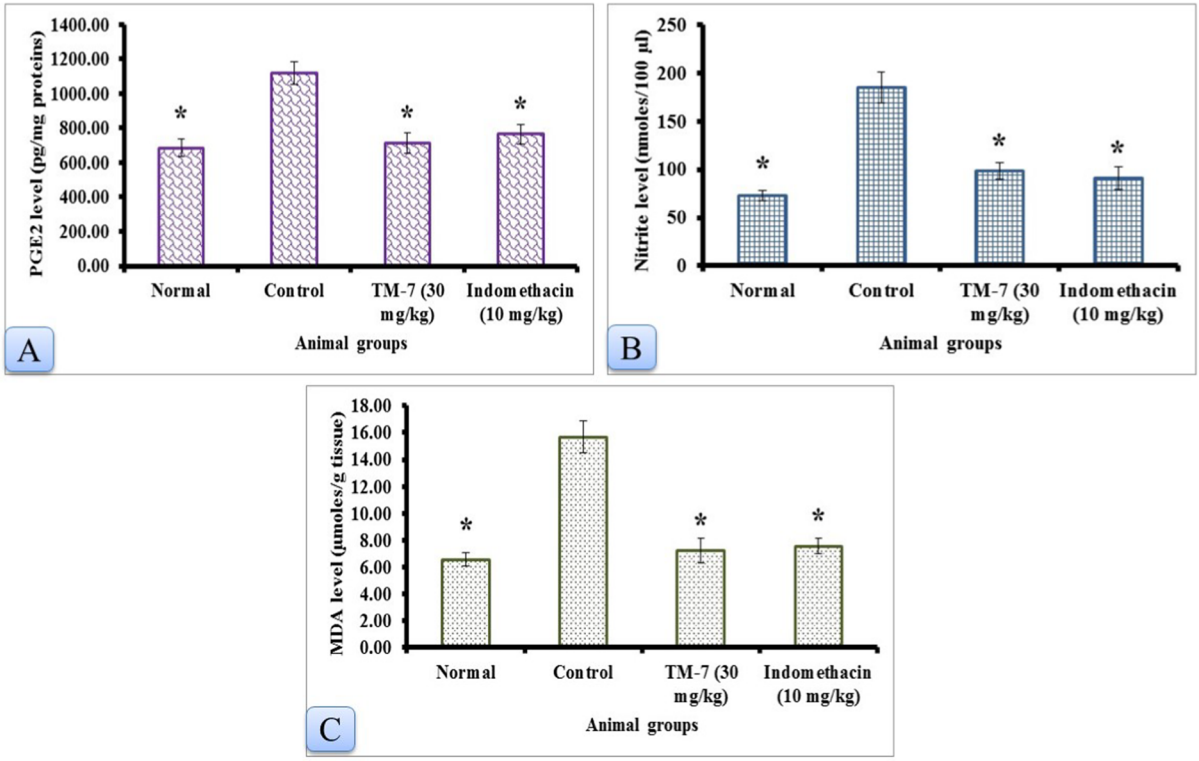

Fig. 5. Effect of TM-7 (30 mg/kg) and indomethacin (10 mg/kg) on PGE2, nitrite, and MDA levels.

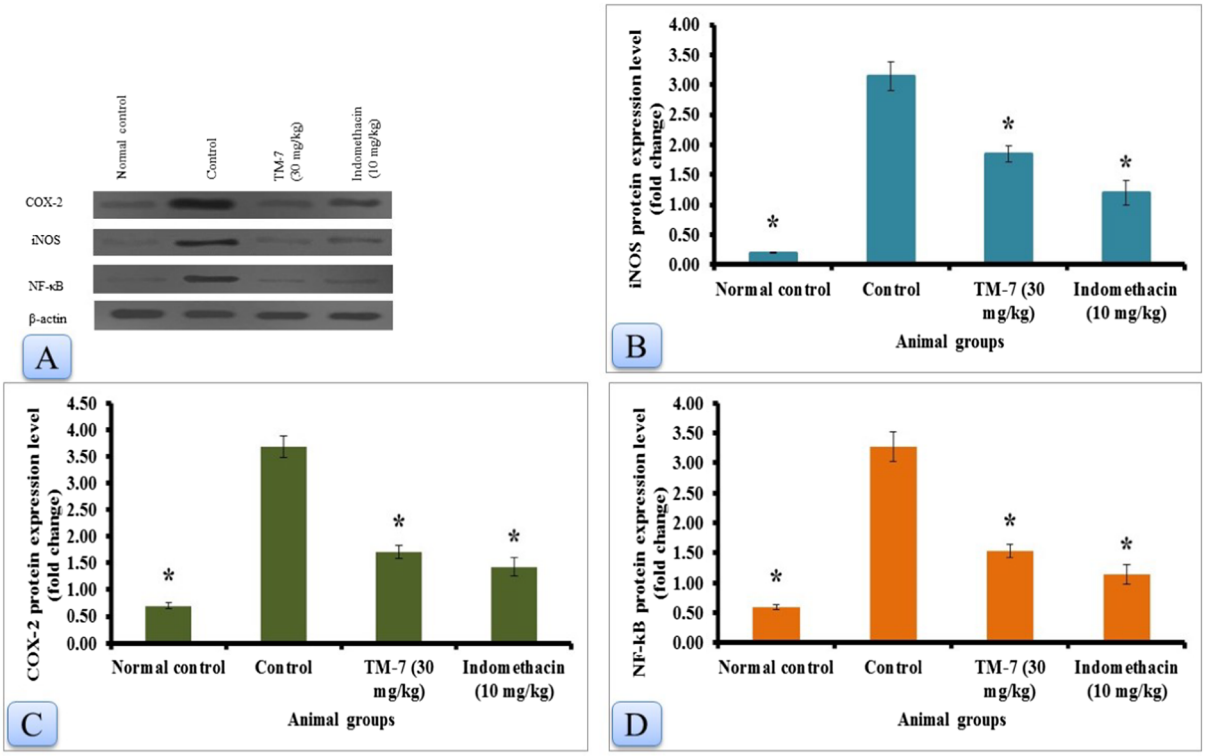

Fig. 6. Effect of TM-7 (30 mg/kg) and indomethacin (10 mg/kg) on COX-2, iNOS, and NF-κB protein expression levels.

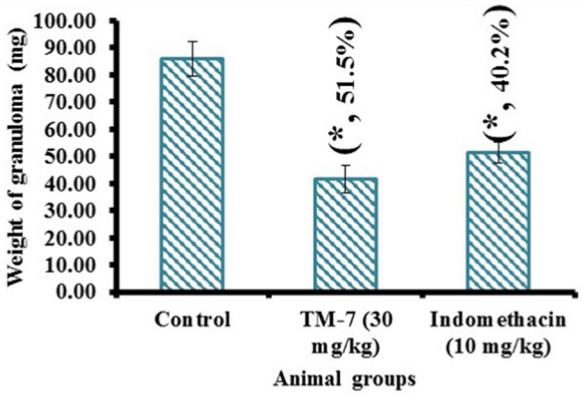

Fig. 7. Anti-inflammatory activity of TM-7 (30 mg/kg) and indomethacin (10 mg/kg) against cotton pellet-induced granuloma model in rats.

added and the mixture was stirred at room temperature. The reaction mixture turns to be cloudy and stirring was continued for another 30 min for complete generation of tetraketone. After complete conversion of the starting materials (as monitored by TLC), 4-nitroaniline and a catalytic amount of acetic acid were added. The reaction mixture was stirred at room temperature for another 24 h. The white tetraketone underwent cyclization reaction with aromatic amine and turns to bright yellow solid. The crude product was transferred to cold water and the solid was washed thoroughly with distilled water and dried under vacuum. The crude nitro functionalized acridinedione (**4**) was carried over to the next step without further purification. Yield: (R_f = 0.73, 1.28 g, 86%); mp 132 °C; FT-IR (KBr, cm^{-1}): 3422 (O—H stretch), 1726 (C═O stretch), 1530 and 1350 (N—O stretch); ^{1}H NMR (400 MHz, DMSO-d_6, ppm) δ_H 0.72–0.86 (m, 12H, Me proton), 1.97–2.21 (m, 8H, CH_2 proton), 4.93 (s, 1H, CH proton), 6.60–6.62 (ABq(d), 2H, Ar, J = 8 MHz), 7.09–7.11 (ABq (d), 2H, Ar, J = 8 MHz), 7.85–7.88 (m, 3H, Ar), 8.39–8.40 (s, 1H, Ar), 9.09 (s, 1H, phenolic OH); ^{13}C NMR (100 MHz, DMSO-d_6) δ_C 26.1, 29.2, 32.1, 40.8, 49.6, 113.7, 114.68, 124.3, 128.5, 136.7, 139.4, 148.6, 149.5, 155.3, 162.5, 195.2; LS-MS (ESI): 486.38 (M^+). Anal. Calcd $C_{29}H_{30}N_2O_5$: C, 71.59; H, 6.21; N, 5.76. Found: C, 71.71; H, 6.18; N, 5.90%.

3.2. Synthesis of amino acridinedione *5*

To a solution of nitroacridiendione (**4**) (1 equiv) in ethanol (7 mL, 3.5 equi) and H_2O (2 mL, 1 equiv), iron powder (325 mesh, 3 equiv) and NH_4Cl (0.6 equiv) were added at room temperature. The reaction mixture was stirred at 85 °C for 1 h, cooled to room temperature, and filtered through celite. The solid was washed thoroughly with ethyl acetate, and then the filtrate was concentrated under reduced pressure and extracted with ethyl acetate. The organic phase was dried over anhydrous $MgSO_4$, filtered, and concentrated. The crude product was purified by flash column chromatography with EtOAc: hexane (1:1, v/v) as eluent affording amino functionalized acridiendione **5**. Yield: (R_f = 0.65, 1.10 g, 94%); mp 76 °C; FT-IR (KBr, cm^{-1}): 3438 (N—H stretch), 3420 (O—H stretch), 3362 (N—H stretch), 1728 (C═O stretch), 1615 (N—H bending); ^{1}H NMR (400 MHz, DMSO-d_6, ppm) δ_H 0.71–0.87 (m, 12H, Me proton), 1.85–2.21 (m, 8H, CH_2 proton), 4.90 (s, 1H, CH proton), 5.51 (br s, 2H, NH_2), 6.45–6.68 (m, 3H, Ar), 6.58–6.60 (ABq(d), 2H, Ar, J = 8 MHz), 7.03–7.05 (ABq (d), 2H, Ar, J = 8 MHz), 7.18 (s, 1H, Ar), 9.10 (s, 1H, phenolic OH); ^{13}C NMR (100 MHz, DMSO-d_6) δ_C 26.1, 29.5, 31.9, 40.1, 49.7, 113.1, 114.5, 126.2, 128.3, 130.1, 137.1, 139.2, 148.9, 150.2, 155.2, 160.6, 195.2; LS-MS (ESI): 456.31 (M^+). Anal. Calcd $C_{29}H_{32}N_2O_3$: C, 76.29; H, 7.06; N, 6.14. Found: C, 76.33; H, 7.15; N, 6.32%.

3.3. Synthesis of isatinimino acridindione *TM-7*

An equimolar mixture of amino acridinedione **5** and isatin **6** in 20 mL of EtOH in the presence of catalytic amount of acetic acid was heated with constant stirring at 90 °C for 1 h. After completing the reaction, monitored by TLC, the reaction mixture was transferred to cold water and the solid was washed thoroughly. The crude product was further purified by flash column chromatography using EtOAc:hexane (8:2 v/v) as eluent yielding isatinimino acridindione (**TM-7**) as yellow

Table 1
In silico molecular docking of TM-7 and Indomethacin with aspirin acetylated human cyclooxygenase-2 (5F19).

Ligand	Protein (PDB ID)	Binding amino acid residues	Binding Energy (kcal/mol)	Inhibition Constant (nM)	VDW_HB desolv_energy (kcal/mol)	Ligand efficiency
TM-7	5F19	Thr'60/O, Arg'61/He, Ser'121/O, Lys'532/Hz2	−8.82	341.7	−10.07	0.20
Indo methacin	5F19	Cys'47/Hn, Tyr'130/Hh, Lys'137/Hz1, Gln'461/2He2	−8.98	263.12	−8.87	0.36

solid. Yield: (R_f = 0.50 in 100% ethyl acetate, 0.95 g, 86%); mp 168 °C; FT-IR (KBr, cm^{-1}): 3427 (O—H stretch), 3382 (amide N—H stretch), 3121 (Ar C—H), 2955 (Aliphatic C—H), 1736 (C═O stretch), 1716 (amide C═O), 1618 (C═N Stretch); ^{1}H NMR (500 MHz, DMSO-d_6, ppm) δ_H 0.64–0.88 (m, 12H, Me proton), 1.84–2.24 (m, 8H, CH_2 proton), 4.88 (s, 1H, CH proton), 6.51–7.36 (m, 12H, Ar), 9.07 (s, OH), 11.03 (s, NH); ^{13}C NMR (125 MHz, DMSO-d_6) δ_C 26.6, 29.9, 32.5, 41.7, 50.1, 111.4, 112.4, 113.7, 115.1, 118.6, 122.4, 128.9, 129.1, 132.3, 135.5, 137.5, 139.0, 140.3, 146.6, 147.8, 149.9, 150.7, 155.7, 163.8, 195.6; LS-MS (ESI): 585.28 (M^+). Anal. Calcd $C_{37}H_{35}N_3O_4$: C, 75.88; H, 6.02; N, 7.17. Found: C, 75.97; H, 6.30; N, 7.29%.

4. Materials and methods

4.1. Animals

Male Wistar albino rats (200–210 g) were used for the current scientific investigation. Animals were maintained on a humidity of 60–70% at nearly 25 ± 1 °C with the 12 h light/dark rotation and have free access to water and diet. All the animal studies were conducted agreeing to the ethical norms permitted by Ministry of Social Justice and Empowerment, Government of India and Institutional Animal Ethics Committee guidelines.

4.2. Carrageenan-induced hind paw oedema in rats

Test drug TM-7 (30 mg/kg) and indomethacin (10 mg/kg) were dissolved in 0.5% CMC and treated orally 1 h earlier carrageenan induction. After that, carrageenan was injected subcutaneously into the right hind paw of rats. Rat hind paw thickness was measured initially and then at 1, 2, 3, 4, and 5 h after the carrageenan injection with digital Vernier calipers [30]. After 5 h, rats were sacrificed and the carrageenan-induced hind paw oedema feet's were dissected and stored at −80 °C until further use.

4.3. Measurement of the tumor necrosis factor α, interleukin 1 β, and IL-6 level in paw tissue

Rat hind paw tissue was homogenized in 500 μl of buffer containing protease inhibitors, and IL-1β, TNF-α, and IL-6 levels were determined using a commercially available ELISA kit (eBioscience, USA) according to the manufacturer instructions.

4.4. Hepatic MDA assay

The MAD level was identified at 532 nm by using the previous method. 1,1,3,3-Tetramethoxypropane was used as standard [31].

4.5. Western blot analysis of iNOS, COX-2 and NFkB

Rat hind paw soft tissues were removed and homogenized by RIPA buffer. The homogenates were centrifuged at 13,000 rpm for 10 min, and 10 μg of total proteins from the supernatants was separated by SDS-PAGE and transferred to polyvinylidene difluoride (PVDF) membranes. The membranes were incubated with anti-iNOS, anti-COX-2, anti-NFkB or anti-β-actin antibodies in 5% skim milk in TBST overnight at 4 °C with 6 rpm. The PVDF membranes were then incubated with horseradish peroxidase-conjugated secondary antibody. The immunoreactive protein bands were detected by the enhanced chemiluminescence (ECL) reagent. ImageJ 1.47 v software (National Institute of Health) was used to quantify the chemiluminescent intensities of protein signals.

4.6. Cotton pellet-induced granuloma in rats

Cotton pellets (35 ± 1 mg) induced granuloma was generated on the axilla region of the rats. Rats were treated by TM-7 (30 mg/kg) or

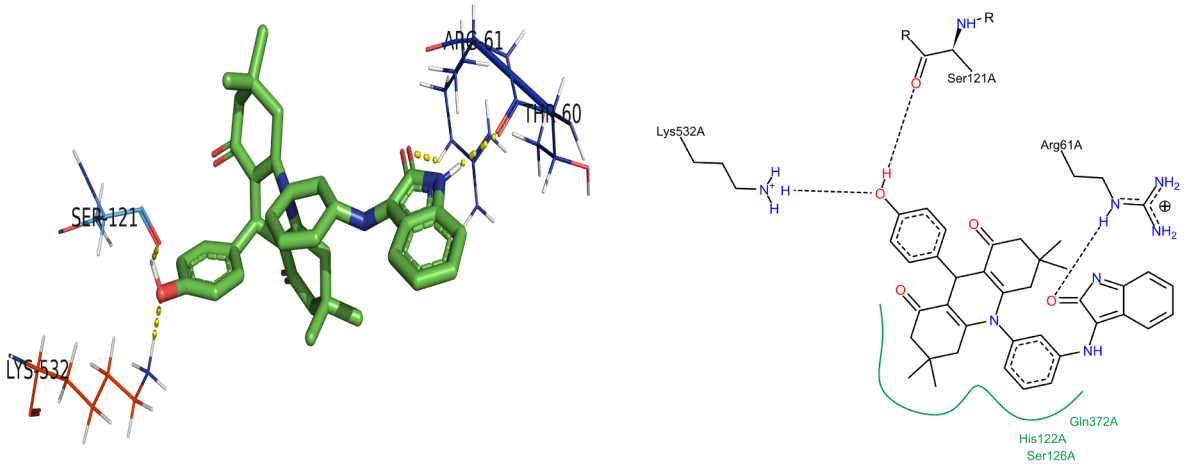

Fig. 8. (a) 3D interaction diagram and (b) 2D interaction diagram of TM-7 with active site of target human cyclooxygenase-2 (5F19). The hydrogen bond interactions are shown as dotted yellow and black lines and the hydrophobic regions are shown in green coloured lines. (For interpretation of the references to colour in this figure legend, the reader is referred to the web version of this article.)

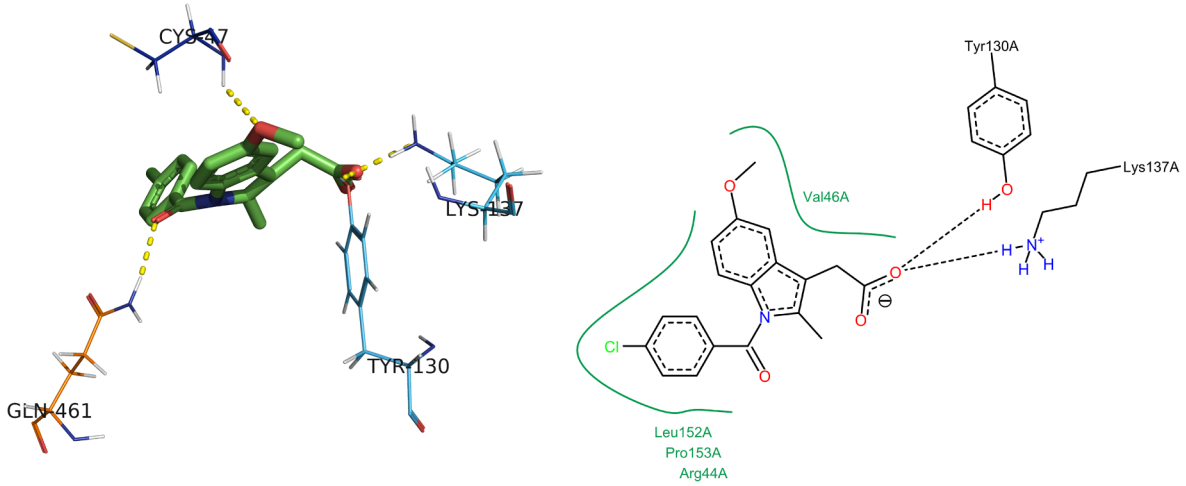

Fig. 9. (a) 3D interaction diagram and (b) 2D interaction diagram of reference drug Indomethacin with active site of target receptor human cyclooxygenase-2 (5F19). The hydrogen bond interactions are shown as dotted yellow and black lines and the hydrophobic regions are shown in green coloured lines. (For interpretation of the references to colour in this figure legend, the reader is referred to the web version of this article.)

indomethacin (10 mg/kg) once a day for seven successive days from the day of cotton pellet grafting. On the 8th day, cotton pellets were removed from animals and dried in a hot air oven at 60 °C. The granuloma level was assessed by subtracting the cotton pellet weight on 0 day from eighth day [32].

4.7. Statistical analysis

The results were expressed as the Mean ± SD. Results obtained from the present study were analyzed using One way ANOVA followed by Tukey's multiple comparison tests. Differences between the data were considered significant at $P < 0.05$.

4.8. In silico molecular docking study

Ligands: The structure of TM-7 and the standard control drug Indomethacin was drawn in ChemDraw Ultra version 12.0 and the connection errors have been checked. Both compounds were optimized and energy minimized using PRODRG server [29] and the low energy confirmation of the selected ligands was docked using AutoDock Tools v 1.5.6. (autodock and autogrid) 4.2 software (http://www.scripps.edu/mb/olson/doc/autodock) and followed by the reported methodology by Stalin et al. [33].

Receptor: The three dimensional X-ray crystal structure of target protein, aspirin acetylated human cyclooxygenase-2 (PDB ID: 5F19) was obtained from the protein data bank (https://www.rcsb.org/structure/5F19). The active sites of the target protein were identified using the CASTp (Computed Atlas of Surface Topography of proteins) server. Based on the target molecules preparation protocol from Autodock, water molecules and hetero groups were deleted from the target enzyme molecules. The target enzyme molecules preparation wizard has been used to assign bond orders, formal charges (Kollman and Gasteiger-type charges), and missing information on connectivity of enzyme structures in PDB.

Docking: Molecular interaction and simulation was performed on the ligand TM-7 and Indomethacin as reference molecule in order to generate superlative pose with highest least score, to reveal its complete accommodation with 5F19 protein active site pocket.

5. Conclusion

In conclusion, the isatinimino acridienedion motif was synthesized successfully with high yield and purity. The results of the present study suggested that the synthesized isatinimino acridiendione showed considerable anti-inflammatory effects in carrageenan-induced hind rat paw oedema, which is equivalent to standard drug indomethacin. The

molecular mechanisms of target molecule might be related to the decline of NF-kB, TNF-α, IL-6, and IL-1β that may possibly result in inhibition of COX-2 and iNOS expression and its product (PGE2 and NO). Our results deliver new perspectives on the therapeutic use of isatinimine acridiendione TM-7 in the management of inflammatory diseases.

Acknowledgements

The authors express their appreciation to the Deanship of Scientific Research at King Saud University for funding this work through research group no. RG-1440-111.

Appendix A. Supplementary material

Experiment details and NMR spectra for synthesized compounds were available in Electronic supplementary information. Supplementary data to this article can be found online at https://doi.org/10.1016/j.bioorg.2019.103047.

References

[1] C. Caruso, D. Lio, L. Cavallone, C. Franceschi, Ann. N. Y. Acad. Sci. 1028 (2004) 1–13.
[2] C.E. Finch, Neurobiol. Aging 26 (2005) 281–291.
[3] H. Rus, F.I. Niculescu, N. Engl, J. Med. 337 (1997) 423–424.
[4] J.P. Gil ligan, S.J. Lovato, M.D. Erion, A.Y. Jeng, Inflammation 18 (1994) 285–292.
[5] Z. Halici, G.O. Dengiz, F. Odabasoglu, H. Suleyman, E. Cadirci, M. Halici, Eur. J. Pharmacol. 566 (2007) 215–221.
[6] D. Ronchetti, V. Borghi, G. Gaitan, J.F. Herrero, F. Impagnatiello, Brit. J. Pharmacol. 158 (2009) 569–579.
[7] R.M. Ion, D. Frackowiak, A. Planner, K. Wiktorowicz, Acta. Biochim. Pol. 45 (1998) 833–845.
[8] S. Isabel, R. Ros, H.C. Daniel, R. Pierre, D.P. Maria, Eur. J. Med. Chem. 41 (2006) 340–352.
[9] S.A. Gamage, N. Tepsiri, P. Wilairat, S.J. Wojcik, D.P. Figgit, R. Ralph, W.A. Denny, J. Med. Chem. 37 (1994) 1486–1494.
[10] S.A. Gamage, D.P. Figgit, S.J. Wojcik, R. Ralph, A. Ransijn, J. Mauel, J. Med. Chem. 40 (1997) 2634–2642.
[11] L.A. Zwelling, S. Michaels, L.C. Erickson, R.S. Ungerleider, M. Nichols, K.W. Kohn, Biochemistry 20 (1981) 6553–6563.
[12] F. Rashedian, D. Saberi, K. Niknam, J. Chin. Chem. Soc. 57 (2010) 998–1006.
[13] Y.-L. Chen, C.-M. Lu, I.-L. Chen, L.-T. Tsao, J.-P. Wang, J. Med. Chem. 45 (2002) 4689–4694.
[14] R. Kumaran, T. Varalakshmi, E.J. Padma Malar, P. Ramamurthy, J. Fluoresc. 20 (2010) 993–1002.
[15] R. Kumaran, P. Ramamurthy, J. Phys. Chem. B 110 (2006) 23783–23789.
[16] R. Kumaran, P. Ramamurthy, J. Lumin. 130 (2010) 1203–1210.
[17] V. Thiagarajan, P. Ramamurthy, Spectrochim. Acta Part A 67 (2007) 772–777.
[18] P. Ashokkumar, V.T. Ramakrishnan, P. Ramamurthy, Eur. J. Org. Chem. 34 (2009) 5941–5947.
[19] R.O. Day, G.G. Graham, Brit. Med. J. 346 (2013) f3195 (1–10).
[20] P. Davidovich, V. Aksenova, V. Petrova, D. Tentler, D. Orlova, S. Smirnov, V. Gurzhiy, A.L. Okorokov, A. Garabadzhiu, G. Melino, N. Barlev, V. Tribulovich, A.C.S. Med, Chem. Lett. 6 (2015) 856–860.
[21] T.R. Bal, B. Anand, P. Yogeeswari, D. Sriram, Bioorg. Med. Chem. Lett. 15 (2005) 4451–4455.
[22] V.R. Solomon, C. Hu, H. Lee, Bioorg. Med. Chem. 17 (2009) 7585–7592.
[23] N. Lashgari, G.M. Ziarani, ARKIVOC i (2012) 277–320.
[24] A.S. Kalgutkar, B.C. Crews, S.W. Rowlinson, A.B. Marnett, K.R. Kozak, R.P. Remmel, L.J. Marnett, Proc. Natl. Acad. Sci. USA 97 (2) (2000) 925–930.
[25] D.-Q. Shi, S.-N. Ni, B.F. Yang, J.-W. Shi, G.-L. Dou, X.-Y. Li, X.-S. Wang, J. Heterocycl. Chem. 45 (2008) 653–660.
[26] G.H. Naik, K.I. Priyadarsini, R.G. Bhagirathi, B. Mishra, K.P. Mishra, M.M. Banavalikar, H. Mohan, Phytother. Res. 19 (2005) 582–586.
[27] Y.Y. Lee, Y.P. Yang, P.I. Huang, W.C. Li, M.C. Huang, C.L. Kao, Y.J. Chen, M.T. Chen, Brain Res. Bull. 116 (2015) 98–105.
[28] M.J. Lucido, B.J. Orlando, A.J. Vecchio, M.G. Malkowski, Biochemistry 55 (2016) 1226–1238.
[29] R.C. Wade, P.J. Goodford, Prog. Clin. Biol. Res. 289 (1989) 433–444.
[30] C.A. Winter, E.A. Risley, G.W. Nuss, Proc. Soc. Exp. Biol. Med. 111 (1962) 544–547.
[31] B. Naghizadeh, M.T. Mansouri, B. Ghorbanzadeh, Y. Farbood, A. Sarkaki, Phytomedicine 20 (2013) 537–542.
[32] C.A. Winter, C.S. Porter, J. Am. Pharm. Sci. 46 (1957) 515–519.
[33] A. Stalin, S.S. Irudayaraj, G.R. Gandhi, K. Balakrishna, S. Ignacimuthu, N.A. Al-Dhabi, Life Sci. 153 (2016) 100–117.